ELSEVIER

Journal of Alloys and Compounds 446–447 (2007) 63–66

Journal of ALLOYS AND COMPOUNDS

www.elsevier.com/locate/jallcom

Hydrogen desorption properties of MgH_2 nanocomposites with nano-oxides and Inco micrometric- and nanometric-Ni

R.A. Varin [a,*], T. Czujko [a], E.B. Wasmund [b], Z.S. Wronski [a,c]

[a] *Department of Mechanical Engineering, University of Waterloo, Waterloo, Ontario, Canada N2L 3G1*
[b] *INCO Special Products, 2101 Hadwen Road, Sheridan Park, Mississauga, Ontario, Canada L5K 2L3*
[c] *Materials Technology Laboratory, CANMET, Natural Resources Canada, 568 Booth Street, Ottawa, Ontario, Canada K1A 0G*

Received 16 September 2006; received in revised form 20 October 2006; accepted 26 October 2006
Available online 1 December 2006

Abstract

The effects of doping with 5 wt.% of nano-oxides (n-Al_2O_3 and n-Y_2O_3), specialty Inco micrometric- and nanometric-Ni (m- and n-Ni) and their equal weight ratio mixtures on the hydrogen desorption properties of commercial MgH_2 were studied. The powder mixtures were mechanically milled for 20 and 100 h. Doping with n-Al_2O_3 does not have a beneficial effect and doping with n-Y_2O_3 has only a limited effect on the temperatures and hydrogen desorption kinetics while nanocomposites doped with specialty Ni show reduced hydrogen desorption temperatures, very fast desorption kinetics under 0.1 MPa H_2 pressure and substantially reduced apparent activation energies of desorption. Prolonged milling for 100 h is detrimental for the hydrogen storage properties of the MgH_2 doped with the specialty Inco m- and n-Ni.

Keywords: Hydrogen absorbing materials; Mechanochemical processing; X-ray diffraction; Kinetics; Differential scanning calorimetry

1. Introduction

Nickel (Ni) improves the hydrogen sorption/desorption kinetics of MgH_2 [1–5]. In particular, a nanostructured Ni either as a single constituent [6,7] or as a component of a nanocomposite comprising nano-Ni, nano-Al_2O_3 and carbon [8] seems to be a very effective catalyst for MgH_2. For some time Inco Special Products (a business unit of Inco Limited) has been manufacturing Type 255^{TM} Ni (referred to hereafter as "micrometric Ni" (m-Ni)) by the nickel carbonyl decomposition process. Type 255^{TM} is an important material for manufacturing sintered plaques and conductive additives in nickel batteries (NiMH and NiCd). Based on the well-established process for Type 255^{TM}, Inco has synthesized a number of experimental batches of much finer specialty Ni powder referred to in this paper as "nanometric Ni" (n-Ni). It has already been found that small additions of these experimental Ni powders greatly improve the rate of the synthesis of MgH_2 by the reactive mechanical milling of elemental Mg under hydrogen [9]. In this work we report the effect of experimental m- and n-Ni batches as well as their nanocomposites with nano-oxides such as nanometric Al_2O_3 and Y_2O_3 (n-Al_2O_3 and n-Y_2O_3), on the hydrogen desorption properties of commercial MgH_2.

2. Experimental

As-received MgH_2 powder (Tego Magnan® from Degussa–Goldschmidt; ~95 wt.%; the remaining Mg) was mixed with 5 wt.% of the additives such as m-Ni (specific surface area 0.7 m^2/g), n-Ni (specific surface area 30.3 m^2/g), n-Al_2O_3 (particle ~10–20 nm) and n-Y_2O_3 (particle ~25 nm) (Alfa Aesar), as well as with 5 wt.% of nanocomposites: (m-Ni + n-Y_2O_3) and (n-Ni + n-Y_2O_3) (equal-weight-ratio of Ni to Y_2O_3). The powder mixtures were mechanically milled for 20 and 100 h under argon (~580 kPa) in a magneto-mill using a very strong impact mode with two Nd–Fe–B magnets (e.g. Refs. [9,10]) and an initial ball-to-powder weight ratio of 55:1. All the powder handling was performed in a purged glove bag under high purity argon. Morphological examination of powders was conducted with a high-resolution, field emission gun scanning electron microscope LEO 1530 by attaching loose powders to stick carbon tape and taking pictures under secondary electron (SE) mode. The powder particle size was calculated from the SEM pictures as the equivalent circle diameter, $ECD = (4A/\pi)^{1/2}$, where A represents the projected particle area, using the Image Tool v.3.00 software. Powders were also characterized by X-ray diffraction (Rigaku Rotaflex D/Max B rotating anode diffractometer using monochromated Cu $K\alpha_1$ radiation with $\lambda = 0.15406$ nm, voltage 55 kV and a current of 180 mA, scan range $2\theta = 10$–90°, scan rate 1.2 $^\circ min^{-1}$ at the step size of 0.02°). The nanograin (crystallite) size of β-MgH_2 in the milled powders was calculated from the broadening of their respective X-ray diffraction (XRD) peaks by

* Corresponding author. Tel.: +1 519 885 1211; fax: +1 519 888 6197.
E-mail address: ravarin@uwaterloo.ca (R.A. Varin).

0925-8388/$ – see front matter © 2006 Elsevier B.V. All rights reserved.
doi:10.1016/j.jallcom.2006.10.134

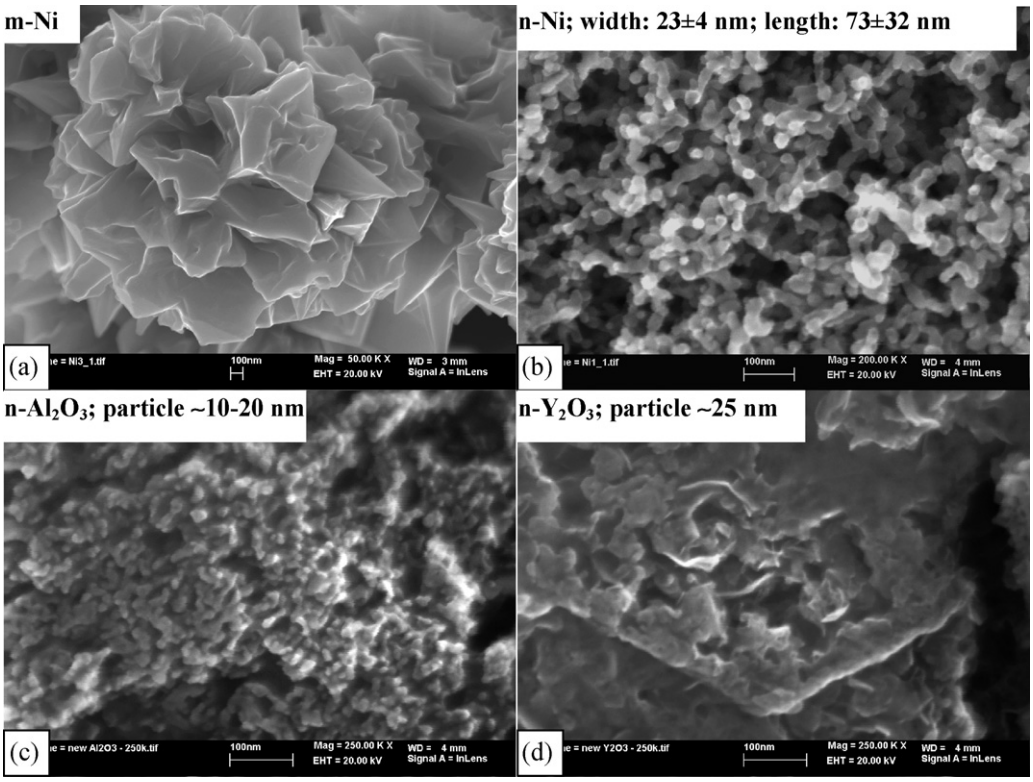

Fig. 1. SEM micrographs of the morphology of additives. (a) micrometric Ni (m-Ni); (b) nanometric Ni (n-Ni); (c) nanometric Al_2O_3 (n-Al_2O_3); (d) nanometric Y_2O_3 (n-Y_2O_3).

separating crystallite size and lattice strain (for details, see for example, Refs. [9,10]). The thermal behavior of powders was analyzed by differential scanning calorimetry (DSC) and the kinetics of hydrogen desorption were evaluated using a volumetric Sieverts-type apparatus custom-built by A.O.C. Scientific Engineering Pty. Ltd., Australia. Desorption was carried out under 0.1 MPa of hydrogen pressure (no prior activation). The calibrated accuracy of desorbed hydrogen capacity is about ±0.2 wt.% H_2 and that of temperature reading ±5 °C (more experimental details can be found in Refs. [9,10]).

3. Results and discussion

The MgH_2 powders used in the mixtures were globular with the mean ECD and XRD grain (crystallite) size of 36 ± 16 μm and ~67 nm, respectively [11]. The micrometric-Ni (m-Ni) (Inco Type 255™) has a macroscopic filamentary shape and at the microscopic level each filament is composed of rose-like corollas joined closely together [9]. Each corolla consists of small petal-like features whose thickness is on the order of or less than ~100 nm (Fig. 1a). The nanometric-Ni (n-Ni) has a filamentary shape resembling a delicate "coral colony" and its dimensions are truly nano with the length of 73 ± 32 nm and diameter of 23 ± 4 nm (Fig. 1b). The nanometric particles of both n-Y_2O_3 and n-Al_2O_3 oxide appear clumped under SEM due to their small size (Fig. 1c and d).

The XRD patterns in Fig. 2 show that after milling for 20 h the microstructure of all the nanocomposite mixtures predominantly consists of β- and γ-MgH_2 hydrides. The latter is a high pressure polymorphic form of β-MgH_2 [12] created due to the localized on-contact impacting action of steel balls on the MgH_2 powder particles in the milling vial [13]. Minor phases observed in the mixture with m-Ni are Ni and Mg_2NiH_4. MgO observed in Fig. 2 forms due to the exposure of residual Mg (~5 wt.% in the as-received MgH_2 powder) to air during powder handling for XRD tests. Identical XRD patterns as those in Fig. 2 were observed for the powders milled for 100 h (not shown here). Fig. 3a and b shows that the milling for 20 h reduced the initial particle size of MgH_2 almost 30-fold (average size less than 1 μm after milling) and crystallite size from the initial ~67 nm to the average ~12 nm. Both the average particle size (ECD) and crystallite (grain) size of β-MgH_2 are independent of the type of additive. No further changes of the ECD and β-MgH_2 crystallite (grain) size were observed after milling for 100 h. Fig. 4 shows that the DSC peak maximum temperature of the MgH_2 powder without additives milled for 20 h is shifted by

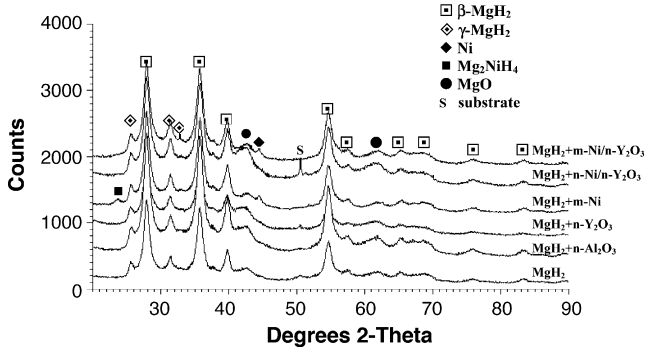

Fig. 2. X-ray diffraction patterns of MgH_2 and nanocomposite mixtures after milling for 20 h.

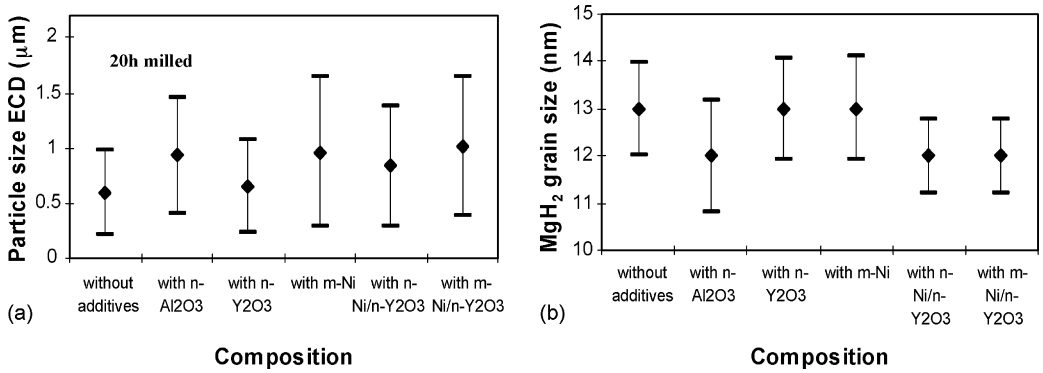

Fig. 3. (a) Particle size (ECD) of nanocomposite mixtures and (b) grain (crystallite) size of β-MgH_2 for the nanocomposite mixtures milled for 20 h.

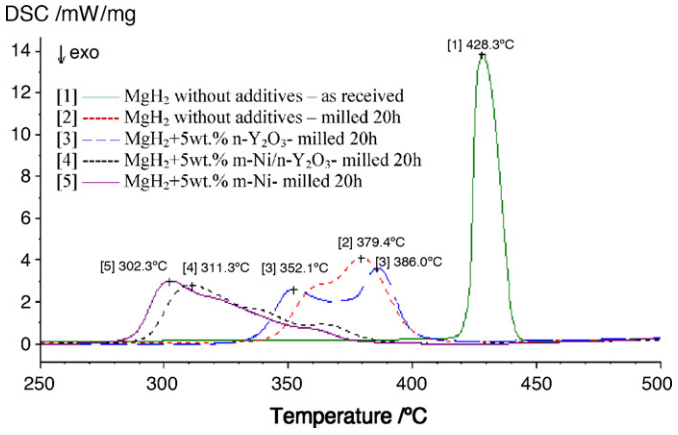

Fig. 4. DSC curves of as-received MgH_2 and MgH_2 and nanocomposite mixtures milled for 20 h.

about 50 °C to the lower temperature range with respect to the as-received powder which is a typical effect of milling due to the formation of γ-MgH_2 and reduction of particle size [11]. It can also be seen that the nano-oxide additives either singly or in the mixture with m-Ni do not have any additional effects on the reduction of the hydrogen desorption temperature. In contrast, the presence of 5 wt.% m-Ni (or n-Ni) reduces the DSC peak maximum temperature of the 20 h milled nanocomposite mixture by ∼80 °C with respect to the as-milled MgH_2 powder and by more than 100 °C with respect to the as-received MgH_2. Milling for 100 h was actually detrimental because the shift of DSC peaks to lower temperature was less than that observed in Fig. 4 for the 20 h milled nanocomposites.

Fig. 5a shows a strong catalytic effect at 275 °C of the Inco m-Ni and slightly lesser of the Inco n-Ni mixed with n-Y_2O_3 on the hydrogen desorption kinetics (under 0.1 MPa H_2 pressure rather than low vacuum) of the non-activated nanocomposite mixtures milled for 20 h. In contrast, the nano-oxides have a substantially lesser effect on improving the kinetics; there is no effect at 275 °C (Fig. 5a), but some intermediate effect at 300 °C (Fig. 5b). The desorption data was analyzed by applying the JMAK (Johnson–Mehl–Avrami–Kolmogorov) theory of phase transformations and the apparent activation energy of desorption was evaluated from the Arrhenius plot as described in [9]. Table 1 shows that the addition of Al_2O_3 does not affect the activation energy. The addition of m-Ni and n-Y_2O_3 by themselves reduces substantially the activation energy of H desorption while the addition of m-Ni and n-Y_2O_3 together does not have a synergistic or additive effect on the activation energy, compared with adding each additive separately. In these experiments, n-Ni was not tested by itself, although this has been done under similar conditions elsewhere [9], and the n-Ni had a similar effect on the activation energy as the m-Ni additive. Finally, it is to be noted that a simple mixing of either the as-received or 20 h milled MgH_2 with the Inco Ni additives did not affect the hydrogen storage properties of the mixtures. Ball milling for an optimized duration is still required.

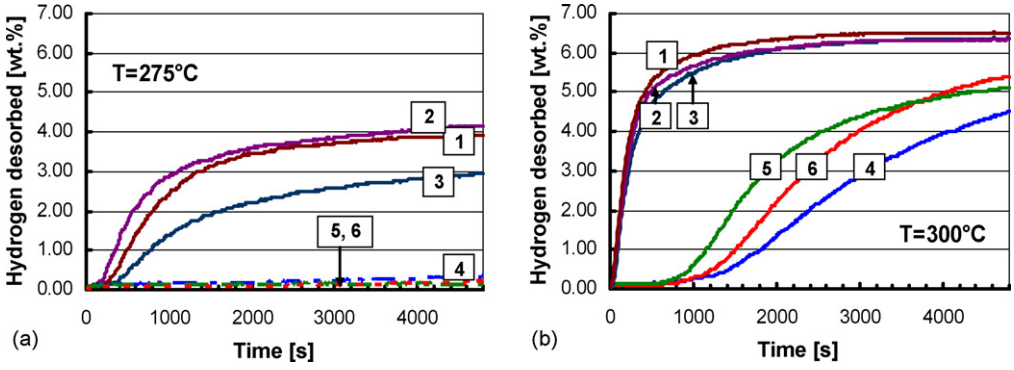

Fig. 5. The kinetics of hydrogen desorption under 0.1 MPa hydrogen pressure without prior activation at (a) 275 °C and (b) 300 °C for the nanocomposite mixtures directly after milling for 20 h. Kinetic curves: 1, m-Ni; 2, m-Ni + n-Y_2O_3; 3, n-Ni + n-Y_2O_3; 4, without additives; 5, n-Y_2O_3; 6, n-Al_2O_3.

Table 1
Apparent activation energy of desorption of powders without and with additives

Powder/additive (5 wt.%)	Apparent activation energy of first desorption, E_A (kJ/mol)		Temperatures used for calculations (°C)
	Milling for 20 h	Milling for 100 h	
MgH_2-Tego Magnan®	140	146	300, 325, 350, 375
n-Al_2O_3	148	146	300, 325, 350, 375
n-Y_2O_3	121	110	300, 325, 350, 375
n-Ni + n-Y_2O_3	118	132	275, 300, 325, 350, 375
m-Ni + n-Y_2O_3	109	120	275, 300, 325, 350, 375
m-Ni	105	121	275, 300, 325, 350, 375

4. Conclusions

Milling of commercial MgH_2 with the nano-oxide additives (Al_2O_3 and Y_2O_3) has a limited effect on improving the hydrogen storage properties. In contrast, the addition of specialty Inco micrometric and nanometric Ni substantially reduces hydrogen desorption temperatures which is also accompanied by very fast desorption kinetics under 0.1 MPa H_2 pressure. The activation energy of desorption is also substantially reduced. Prolonged milling for 100 h is detrimental for the hydrogen storage properties of the m- and n-Ni-doped MgH_2. Optimization of milling time is still required.

Acknowledgements

This work was financially supported by a grant from the Natural Sciences and Engineering Research Council of Canada which is gratefully acknowledged. The authors would like to thank Steve Baksa of Inco Technical Ltd. for producing some of the nanoscale nickel powders.

References

[1] J. Huot, E. Akiba, T. Takada, J. Alloys Compd. 231 (1995) 815–819.
[2] P. Tessier, E. Akiba, J. Alloys Compd. 293–295 (1999) 400–402.
[3] G. Liang, J. Huot, S. Boily, A. Van Neste, R. Schulz, J. Alloys Compd. 292 (1999) 247–252.
[4] S. Doppiu, P. Solsona, T. Spassov, G. Barkhordarian, M. Dornheim, T. Klassen, S. Suriñach, M.D. Baró, J. Alloys Compd. 404–406 (2005) 27–30.
[5] S. Doppiu, L. Schultz, O. Gutfleisch, J. Alloys Compd. 427 (2007) 204–208.
[6] N. Hanada, T. Ichikawa, H. Fujii, J. Alloys Compd. 404–406 (2005) 716–719.
[7] N. Hanada, T. Ichikawa, H. Fujii, J. Phys. Chem. B 109 (2005) 7188–7194.
[8] Y. Kojima, Y. Kawai, T. Haga, J. Alloys Compd. 424 (2006) 294–298.
[9] R.A. Varin, T. Czujko, E.B. Wasmund, Z.S. Wronski, J. Alloys Compd. 432 (2007) 217–231.
[10] R.A. Varin, S. Li, Z. Wronski, O. Morozova, T. Khomenko, J. Alloys Compd. 390 (2005) 282–296.
[11] R.A. Varin, T. Czujko, Z. Wronski, Nanotechnology 17 (2006) 3856–3865.
[12] J.-P. Bastide, B. Bonnetot, J.M. Létoffé, Mater. Res. Bull. 15 (1980) 1779–1787.
[13] J. Huot, G. Liang, S. Boily, A. Van Neste, R. Schulz, J. Alloys Compd. 293–295 (1999) 495–500.